arXiv:cond-mat/0311093v1 5 Nov 2003

On-surface and Subsurface Adsorption of Oxygen on Stepped Ag(210) and Ag(410) Surfaces

A. Kokalj[a,b], N. Bonini[a] *, A. Dal Corso[a],
S. de Gironcoli[a] and S. Baroni[a]

[a] *SISSA–Scuola Internazionale Superiore di Studi Avanzati and INFM DEMOCRITOS National Simulation Center, I-34014 Trieste, Italy*

[b] *Jožef Stefan Institute, SI-1000 Ljubljana, Slovenia*

Abstract

The adsorption of atomic oxygen and its inclusion into subsurface sites on Ag(210) and Ag(410) surfaces have been investigated using density functional theory. We find that—in the absence of adatoms on the first metal layer—subsurface adsorption results in strong lattice distortion which makes it energetically unfavoured. However subsurface sites are significantly stabilised when a sufficient amount of O adatoms is present on the surface. At high enough O coverage on the Ag(210) surface the mixed on-surface + subsurface O adsorption is energetically favoured with respect to the on-surface only adsorption. Instead, on the Ag(410) surface, at the coverage we have considered (3/8 ML), the existence of stable terrace sites makes the subsurface O incorporation less favourable. These findings are compatible with the results of recent HREEL experiments which have actually motivated this work.

Key words: Density functional calculations, Catalysis, Silver, Oxygen, Stepped single crystal surfaces.

1 Introduction

The interaction between oxygen and silver surfaces has been the subject of extensive experimental and theoretical research because of its key role in important heterogeneous catalytic reactions, such as partial oxidation of methanol to

* Corresponding Author. Phone: +39-040 3787477, Fax: +39-040-3787528.
Email address: bonini@sissa.it (N. Bonini[a]).

formaldehyde or ethylene epoxidation [1]. Despite significant efforts, these systems are still not well understood and the identification of the active species involved in these reactions remains unclear. In particular, defect sites and subsurface oxygen species have attracted considerable attention since they are believed to be important in the ethylene epoxidation reaction [2].

In recent experimental works [3,4,5] Rocca and coworkers have investigated the interaction of oxygen with Ag(410) and Ag(210) surfaces with the aim of understanding the role of steps in the adsorption of oxygen on silver. In particular, using a supersonic molecular beam to dose oxygen on the surface and characterising the final adsorption state by vibrational spectroscopy (HREEL), they have studied the different oxygen species which form on these surfaces. Of particular interest are the results for O/Ag(210) [5]. The HREEL spectra of this system show a peak around 56 meV which is proposed to be due to the vibration of an oxygen atom occupying a subsurface site. Such a peak appears only when preadsorbed oxygen is present on the surface and it is not observed neither on low Miller index surfaces nor on O/Ag(410).

Motivated by these results we have performed an *ab initio* calculation to investigate the possibility of incorporating oxygen into interstitial subsurface sites on Ag(210) and Ag(410) surfaces.

Recent theoretical works have studied the inclusion of O into subsurface regions of low Miller index silver surfaces, i.e. Ag(111) [6] and Ag(100) [7]. It was found that pure subsurface O atoms are always unstable with respect to the oxygen molecule but the presence of co-adsorbed on-surface O atoms can stabilise them. More generally, we find that the adsorption in subsurface sites depends significantly on coverage. Isolated subsurface oxygen atoms are always less stable than adatoms occupying favourable on-surface sites, essentially because of the high energy cost for lattice distortion induced by subsurface O incorporation. However, increasing the coverage the preference of on-surface sites decreases and, for example, in O/Ag(111) pure subsurface sites are stabilised at coverages higher than 0.5 ML [6]. This behaviour is due to the fact that the repulsive interaction between the adsorbates is more effectively shielded for the subsurface atoms than for the on-surface ones. In this work we consider high Miller index surfaces in order to investigate the effects of steps on the incorporation of oxygen atoms into subsurface sites.

2 Computational Details

Calculations were performed in the framework of density functional theory (DFT) using the generalised gradient approximation (GGA) of Perdew-Burke-Ernzerhof (PBE) [8]. We have used the pseudopotential method with ultra-soft

pseudopotentials [9] and plane-wave basis sets up to a kinetic-energy cutoff of 27 Ry (216 Ry for the charge-density). Details about the Ag and O pseudopotentials are reported in Ref. [10]. Brillouin zone (BZ) integration has been performed with the Gaussian-smearing special-point technique [11,12] with a smearing parameter of 0.03 Ry. Calculations have been done using the `PWscf` package [13], while the molecular graphics were produced by the `XCRYSDEN` [14] graphical package.

We have used periodic super-cells as models of the surface. The Ag(210) surface is modelled with slab of 14 (210) layers, which corresponds to seven (100) layers rotated by an angle ϕ_2 ($\tan(\phi_2) = 1/2$) around the [001] axis and merged together so as to form the Ag(210) surface. The Ag(410) is modelled with slabs of 20 (410) layers corresponding to five (100) layers rotated by an angle ϕ_4 ($\tan(\phi_4) = 1/4$) and merged together. Adjacent slabs are separated by a vacuum region of at least 16 a.u. Oxygen is adsorbed on both sides of the slab and all the structures have been fully relaxed until the Hellmann-Feynman forces were lower than 10^{-3} Ry/a.u.

Adsorption of atomic oxygen has been modelled by (2×1) surface super-cells. For the Ag(210) surface the BZ integrations have been performed using a (4×7×1) Monkhorst-Pack mesh, while for the Ag(410) surface a $(4 \times 4 \times 1)$ mesh has been applied. All the calculations are non-spin-polarised, because the interaction between O and the Ag substrate results in a negligible spin moment on the O atom.

The chemisorption energies, $\overline{E}_{\rm chem}$, are referred to the clean Ag(n10) surface ($n = 2, 4$) and the isolated oxygen molecule, $\overline{E}_{\rm chem} = (E_{\rm O/Ag} - E_{\rm Ag} - N_{\rm O}(E_{\rm O_2}/2))/N_{\rm O}$, where the total energy of the adsorbate–substrate system, of the clean surface, of the isolated O_2 molecule, and the number of adsorbed oxygen atoms are represented by $E_{\rm O/Ag}$, $E_{\rm Ag}$, $E_{\rm O_2}$ and $N_{\rm O}$, respectively. $E_{\rm O_2}$ is estimated from a spin-polarised calculation. With this definition, stable adsorbates have negative chemisorption energies.

3 Results and Discussion

In previous works on Ag(001) [10,15], we found that the surface four-fold hollow site is the most stable one and the chemisorption energy was found to decrease increasing the coverage, a fact related to the repulsive lateral electrostatic interaction between negatively charged oxygen adatoms. Recently, we performed a systematic study of on-surface atomic oxygen adsorption on Ag(410) and Ag(210) surfaces [16]. Figure 1 shows the structure of the two surfaces and the on-surface sites that have been studied. In site A the oxygen adatom lies just above the step and is coordinated with three Ag surface

atoms; in site B the oxygen adatom lies in the hollow site just below the step. These two sites are present on both surfaces. The Ag(410) surface possesses also the T_1 and T_2 sites (see Figure 1) with the O adatom in the four-fold hollow sites on the (100) terrace. We find that the configuration in which the adatoms occupy the sites A forming –O–Ag–O–Ag– rows (configuration labelled A–A) is particularly stable. On the Ag(210) surface the step decoration is significantly more favourable than the other adsorption configurations. On Ag(410), instead, the terrace sites have a chemisorption energy almost degenerate with that of the step sites. In particular, on this surface, when the adatoms are far apart from each other the hollow sites on terrace are slightly more stable than the step edge sites, while at higher coverage the adatoms slightly prefer to decorate the steps.

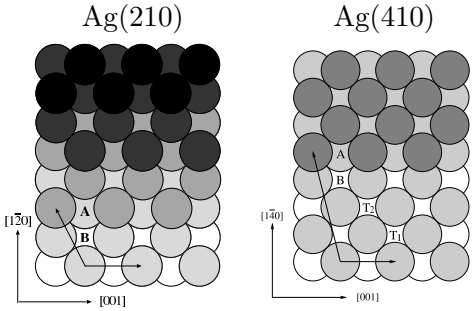

Fig. 1. Schematic representation of the Ag(210) (left) and Ag(410) surface (right). The labels A, B, T_1 and T_2 indicate different adsorption sites: A, above the step; B, below the step; T_1 and T_2, hollow sites on terrace. The surface unit-cell vectors, and the [001] and $[1\bar{n}0]$, $n = 4, 2$, crystal axes are also shown.

Let us focus now on the energetics of oxygen inclusion into subsurface interstitial sites, addressing in particular the effects of on-surface co-adsorption. Our results are summarised in Table 1 and discussed in the next paragraphs.

The inclusion of oxygen into subsurface sites is strongly unfavourable with respect to on-surface O adsorption, the resulting chemisorption energies on Ag(210) surface being as low as -0.07 eV for subsurface-octahedral site (Octa) and -0.14 eV for subsurface-tetrahedral site (Tetra).[1] It is interesting to observe that the adsorption in Octa and Tetra sites on Ag(100) at $\theta = 0.25$ ML [7] is considerably less stable (0.79 eV and 0.69 eV, respectively) than on Ag(210) surface. This indicates that the presence of steps induces a stabilisation of subsurface oxygens. In the right panels of Figure 2 we show top views of the optimised structures with O atom in the Octa and Tetra sites. Note that due to a significant distortion of the substrate lattice induced by subsurface O atoms, the surface structure of Ag(210) can hardly be recognised. However these subsurface sites are significantly stabilised when a

[1] These calculations were performed with Ag slabs composed of only 10 (210)-layers and somewhat smaller $(3 \times 5 \times 1)$ Monkhorst-Pack mesh.

Table 1
Average chemisorption energies, $\overline{E}_{\rm chem}$, for purely subsurface, mixed on-surface + subsurface, and on-surface only adsorption of atomic oxygen on Ag(210) and Ag(410) surfaces. The label of OCTA, TETRA, A, B, and T_1 are defined in text.

Surface	Coverage	Configuration	$\overline{E}_{\rm chem}$(eV)
Ag(210)			
	$\theta = 1/4$ ML	OCTA	-0.07
		TETRA	-0.14
		A	-0.68
	$\theta = 3/4$ ML	A–A + OCTA	-0.54
		A–A + B	-0.40
Ag(410)			
	$\theta = 3/8$ ML	A–A + OCTA	-0.55
		A–A + B	-0.68
		A–A + T_1	-0.63

sufficient amount of O adatoms is present on the surface. The chemisorption energies for A–A+OCTA configuration [2] are -0.54 and -0.55 eV for Ag(210) and Ag(410) surfaces, respectively. Also observe that the substrate reconstruction is considerably reduced in these cases, and that the Ag(210) and Ag(410) surface structures can be easily recognised from the corresponding optimised O/Ag structures (see left panel of Fig 3 and right panel of Fig 4).

It is interesting to compare the stability of mixed on-surface + subsurface configurations with the purely on-surface ones at a given (high enough) oxygen coverage. In all the configurations we have considered, O adatoms decorate the step-edge (A–A arrangement). An additional oxygen atom is then considered to be located either into subsurface OCTA site (A–A+OCTA) or adsorbed on a given surface hollow site (see Figs 3 and 4). For Ag(210), we consider only the A–A+B configuration with an additional O adatom located in the on-surface hollow B site situated below the step edge. For Ag(410), in addition to the A–A+B geometry, we also consider the configuration with an additional O atom adsorbed on the terrace T_1 site (configuration A–A+T_1). On Ag(210) the mixed on-surface + subsurface A–A+OCTA configuration is more stable than the pure on-surface A–A+B configuration, $\overline{E}_{\rm chem}$ being -0.54 and -0.40 eV, respectively. On the contrary, the opposite is true for the Ag(410) surface, where the chemisorption energies for the A–A+OCTA and A–A+B configurations are -0.55 and -0.68 eV, respectively. This qualitative difference is related to the different O coverages of the two surfaces, which is larger on Ag(210) surface ($\theta = 3/4$ ML) than on Ag(410) ($\theta = 3/8$ ML).

[2] In this configuration O adatoms decorate the step-edge and an additional O atom per (2×1) super-cell is located into OCTA site situated straightly below a step-edge Ag atom.

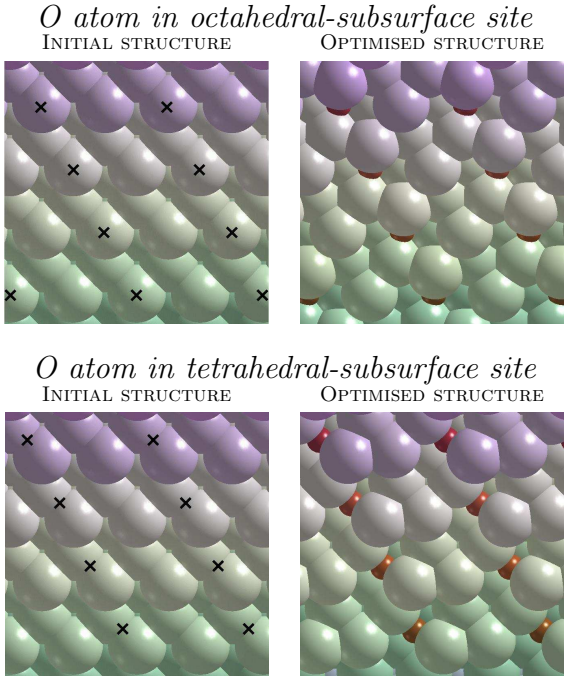

Fig. 2. Oxygen atoms located in subsurface sites on Ag(210) surface. Large (small) balls are silver (oxygen) atoms. On left-side panels the horizontal positions of subsurface-octahedral (Octa) (top left panel) and subsurface-tetrahedral (Tetra) (bottom left panel) sites are marked with crosses (×), while vertically these sites are located below the first layer Ag atoms in the octahedral and tetrahedral interstices. On right-side panels the corresponding optimised O/Ag structures are shown. Note a significant distortion of the substrate lattice—the (210) surface-structure attributes can hardly be recognised.

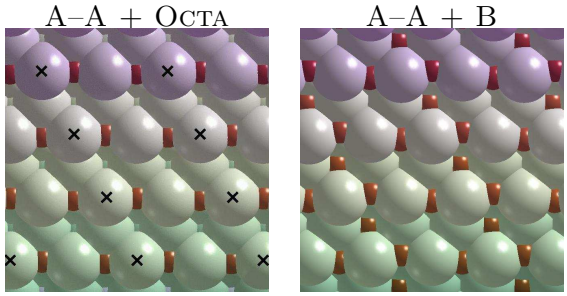

Fig. 3. The two competing O/Ag(210) structures at $\theta = 3/4$ ML oxygen coverage. On both structures the oxygen atoms are decorating the step-edge (A–A). On the left structure an additional oxygen per (2×1) super-cell is located in the subsurface-octahedral site (Octa), i.e., O atoms located straightly below the marked (×) step Ag atoms in octahedral interstices. On the right structure the additional O atom per (2×1) super-cell is located in the hollow site below the step-edge (B).

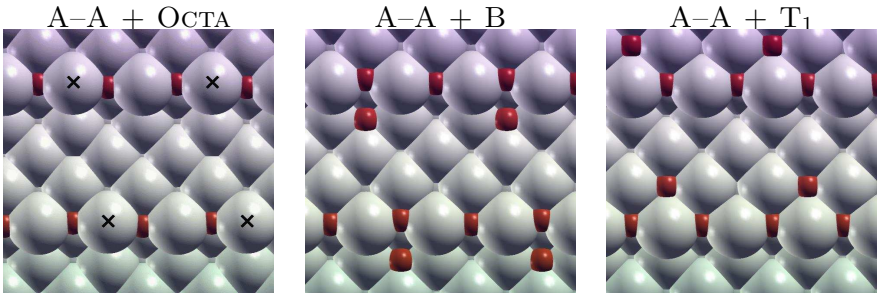

Fig. 4. The O/Ag(410) structures at $\theta = 3/8$ ML oxygen coverage. From left to right: A–A + Octa, A–A + B and A–A + T_1. For the A–A + Octa structure the Octa-oxygen atoms are located straightly below the marked (×) step Ag atoms in octahedral interstices.

This suggests that the electrostatic repulsion between the adsorbates in the A–A+B configuration is stronger on Ag(210) than on Ag(410) and makes this geometry on Ag(210) significantly less favourable. Also note that the effect of high coverage in Ag(210) is weaker for the A–A+Octa configuration essentially because the distance between the adatoms is larger than in the A–A+B arrangement and because the interaction involving subsurface O species is shielded more effectively than for purely on-surface O atoms. In addition to this, we have found that on Ag(410) the incorporation of oxygen into subsurface sites is less stable than on-surface adsorption also because of the availability of stable terrace sites. The A–A+T_1 configuration is indeed more stable than the A–A+Octa one.

4 Conclusions

Our results are compatible with the suggestion, put forward in Ref. [5], that the HREELS peak found at 56 meV in Ag(210), and missing in Ag(410), is due to atomic oxygen adsorbed subsurface. Indeed our calculations, although performed at different coverages, indicate that subsurface O is not stable in Ag(410), while it is stabilised in Ag(210) at high enough coverage. Further theoretical investigations spanning a larger range of coverages are called for. Lattice vibrational calculations on selected O/Ag(n10) configurations would probably fully clarify the picture.

Acknowledgements

This work has been supported by INFM (*Iniziativa trasversale calcolo parallelo, Sezioni F e G*) and by the Italian MIUR (PRIN). All numerical calculations were performed on IBM-SP3 and IBM-SP4 computers at CINECA in

Bologna (Italy).

References

[1] R. A. van Santen, H. P. C. E. Kuipers, Adv. Catal. 35 (1987) 265.

[2] P.J. Van den Hoek, E.J. Baerends and R.A. Van Santen, J. Phys. Chem. 93 (1989) 6469.

[3] L. Savio, L. Vattuone and M. Rocca, Phys. Rev. Lett. 87 (2001) 276101.

[4] L. Savio, L. Vattuone and M. Rocca, J. Phys. Condens. Matter 14 (2002) 6065.

[5] L. Vattuone, L. Savio and M. Rocca, Phys. Rev. Lett. 90 (2003) 228302.

[6] W.X. Li, C. Stampfl, M. Scheffler, Phys. Rev. B 67 (2003) 045408.

[7] G. Cipriani, Ph.D. Thesis, SISSA, Trieste, 2000; M. Gajdos, A. Eichler, J. Hafner, SS531 (2003) 272.

[8] J. P. Perdew, K. Burke, M. Ernzerhof, Phys. Rev. Lett. 77 (1996) 3865.

[9] D. Vanderbilt, Phys. Rev. B 41 (1990) 7892–7895.

[10] G. Cipriani, D. Loffreda, A. Dal Corso, S. de Gironcoli, S. Baroni, SS501 (2002) 182–190.

[11] H. J. Monkhorst, J. D. Pack, Phys. Rev. B 13 (1976) 5188.

[12] M. Methfessel, A. T. Paxton, Phys. Rev. B 40 (1989) 3616.

[13] S. Baroni, A. Dal Corso, S. de Gironcoli, P. Giannozzi, PWscf and PHONON: Plane-wave pseudo-potential codes, http://www.pwscf.org/ (2001).

[14] A. Kokalj, J. Mol. Graphics Modelling 17 (1999) 176–179. A. Kokalj, M. Causà, XCrySDen: (X-window) CRYstalline Structures and DENsities, http://www.xcrysden.org/ (2003).

[15] D. Loffreda, A. Dal Corso, S. Baroni, L. Savio, L. Vattuone, M. Rocca, SS530 (2003) 26.

[16] N. Bonini, A. Kokalj, A. Dal Corso, S. de Gironcoli, S. Baroni, unpublished.